Gut epithelial and vascular barrier abnormalities in patients with chronic intestinal pseudo-obstruction

Elisa Boschetti[1,#], **Anna Accarino**[2,#], **Carolina Malagelada**[2,#], **Juan R. Malagelada**[2], **Rosanna F. Cogliandro**[1], **Alessandra Gori**[1], **Vitaliano Tugnoli**[3], **Fiorella Giancola**[1], **Francesca Bianco**[1], **Elena Bonora**[1], **Paolo Clavenzani**[4], **Umberto Volta**[1], **Giacomo Caio**[5], **Catia Sternini**[6], **Vincenzo Stanghellini**[1,§], **Fernando Azpiroz**[2,§], and **Roberto De Giorgio**[5,§,*]

[1]Department of Medical and Surgical Sciences, University of Bologna, Bologna, Italy

[2]Digestive System Research Unit, University Hospital Vall d'Hebron; Centro de Investigación Biomédica en Red de Enfermedades Hepáticas y Digestivas (CIBERehd)

[3]Department of Biomedical and Neuro Motor Sciences, University of Bologna, Bologna, Italy

[4]Department of Veterinary Medicine, University of Bologna, Ozzano, Italy

[5]Department of Medical Sciences, University of Ferrara, Ferrara, Italy

[6]Digestive-Disease-Division, Departments of Medicine and Neurobiology, David Geffen School of Medicine, University of California Los Angeles (UCLA), Los Angeles, USA.

Abstract

Background: Chronic-intestinal-pseudo-obstruction (CIPO) is a rare condition due to severe impairment of gut motility responsible for recurrent sub-occlusive episodes. Although neuro-muscular-glial-ICC abnormalities represent the main pathogenetic mechanism, the pathophysiology of CIPO remains poorly understood. Intestinal epithelial and vascular-endothelial barrier (IEVB) abnormalities can contribute to neuro-epithelial changes by allowing passage of harmful substances.

Methods: To test retrospectively whether IEVB defects occur in patients with CIPO we measured the jejunal protein expression of the major tight junction (TJ) components. CIPO patients were subdivided according to gut neuromuscular histopathology: apparently normal (AN); with

*Corresponding Author: Roberto De Giorgio, Department of Medical Sciences, Internal Medicine Unit, University of Ferrara, St. Anna Hospital, Via A. Moro, 8 - 44124 Cona, Ferrara, Italy, Tel.: +39 - 0532 - 236.631 - dgrrrt@unife.it.

inflammation (INF); or with degenerative alterations (DEG). The presence of occludin/claudin oligomers (index of TJ assembly), the amount of occludin, claudin-4 and *zonula occludens*-1 (ZO-1), as well as the expression of vasoactive intestinal polypeptide (VIP) and glial fibrillary acidic protein (GFAP) immunoreactivities were evaluated on jejunal full thickness biopsies using Western Blot.

Key Results: Oligomers were absent in the 73% of CIPO. Total occludin decreased in CIPO with AN and INF changes. Claudin-4 was upregulated in CIPO with INF and DEG features. ZO-1 and VIP expression decreased selectively in DEG group. GFAP increased in CIPO regardless the histopathological phenotype.

Conclusions & Inferences: The absence of oligomers demonstrated in our study suggests that IEBV is altered in CIPO. The mechanism leading to oligomerization is occludin-dependent in AN and INF, whereas is ZO-1-dependent in DEG. Our study provides support to IEVB abnormalities contributing to CIPO clinical and histopathological features.

Summary

The study aim to test retrospectively whether the intestinal epitelial and vascular barriers (IEVB) defects may occur in patients with chronic-intestinal-pseudo-obstruction (CIPO), thus playng a role in CIPO phisiophatology.

We dempnstrated abnormalities to protein expression and aggregation of major tight junction (TJ) components in the jejunum of CIPO patients suggesting that IEVB integrity is compromised in this condition.

We propose that IEVB changes may contribute to neuro-ICC-muscular abnormalities in symptoms / manifestations detectable in CIPO patients. The identified molecular targets may be exploitable to design treatment options for patients with severe gut dysmotility

1. INTRODUCTION

Chronic-intestinal-pseudo-obstruction (CIPO) is a rare gastrointestinal (GI) motility disorder mimicking a mechanical obstruction.[1–3] CIPO is responsible for significant morbidity, poor quality of life and even mortality,[4, 5] thus representing the "tip of the iceberg" of severe gut dysmotility[6] Histopathological analysis of gut specimens usually show neuro-interstitial cells of Cajal (ICC)-muscular abnormalities, with or without an inflammatory infiltrate.[4, 7–9] Even if these alterations represent the primary pathophysiologic mechanisms underlying CIPO[4, 7–9], we hypothesized that molecular abnormalities to tight junctions (TJ) expressed throughout the intestinal epithelial or vascular-endothelial lining might also play a role in the pathogenesis of this condition. TJ integrity is crucial to prevent a 'leaky gut', which would allow injurious molecules to permeate the intestinal epithelium and/or the vascular endothelium. Alterations occurring independently to one of the two barriers are known to contribute to a variety of pathological conditions, such as inflammatory and functional

bowel disorders, although their role in CIPO pathophysiology and clinical manifestations remain to be elucidated. Recent evidence demonstrates that when one of the two barriers is altered the permeability is also increased.[10] For this reason, we will consider the two barriers like a sort of single, TJ integrity-related unit referred to as intestinal epithelial and vascular barrier (IEVB).

Tight junctions (TJs) represent the first key structure of IEVB and are composed of a group of intramembranous multiprotein complexes holding together adjacent enterocytes or contiguous vascular endothelial cells.[10] This system generates a selective physical barrier to paracellular diffusion. TJs are composed of transmembrane proteins, i.e. occludin (OCLN) and claudins (CLDNs) that interact with cytoplasmic accessory, signaling, and regulatory proteins to form a barrier capable of rapid assembly and disassembly in response to stimuli; and cytoplasmic adaptor proteins, i.e. *zonula occludens*-1 (ZO-1), that mediate the connection between the transmembrane complex and the cytoskeleton.[11–18] Various mechanisms regulate TJ function and growing knowledge indicates that a defective paracellular sealing/transport via IEVB may play a role in a wide array of inherited and acquired human diseases.[19]

OCLN-CLDNs oligomerization forms the TJ selective pore which directly determine the paracellular permeability.[11][12, 13, 20, 21] The CLDN family encompasses 24 isoforms that are expressed in a tissue-specific manner.[14] Each CLDN have its own intrinsic paracellular selectivity, thus the overall TJ selectivity depends on the combination of the cell background and the expressed CLDNs.[15] Among the large CLDN family, CLDN4 is highly expressed along the GI tract from the duodenum to the colon and is altered in several GI diseases such as, ulcerative colitis, irritable bowel syndrome and microscopic colitis.[16] Finally, ZO-1 is a cytoplasmic protein that stabilizes the IEVB by linking OCLN/CLDNs pore to actin-myosin cytoskeleton.[17] ZO-1 also controls the spatial distribution of CLDNs.[18]

The enteric nervous system exerts a crucial role in tuning TJ assembly/disassembly in normal condition. [2][28] In particular, IEVB homeostasis has been shown to be regulated by submucosal neurons containing vasoactive intestinal polypeptide (VIP)[8, 22, 23] as well as enteric glia.[24] In order to gain insight into the role of IEVB /TJ abnormalities in CIPO, we designed the present retrospective study to test whether there are 1) IEVB /TJ abnormalities in CIPO by analyzing OCLN/CLDNs oligomeric assembly (as markers of IEVB integrity) and the expression of major TJs components, i.e. OCLN, CLDN4, ZO-1; and 2) changes in the expression of VIP, and glial cell activation by measuring intermediate filament glial fibrillary acidic protein (GFAP).[25]

2.   Materials and Methods

2.1   Patients and sampling

Full-thickness jejunal samples were collected from n=22 well characterized CIPO patients (12 females; age range: 16–77 years) at the Vall d'Hebron Hospital (Barcelona, Spain) during a six year period (from 2010 to 2016). Comparable jejunal samples used as control tissues were obtained from n=7 (3 females; age-range: 48–73 years) patients undergoing resection due to non-complicated GI tumors. Patients with motility disorders secondary to

infectious, neurological, metabolic, systemic-autoimmune, and paraneoplastic conditions were excluded. Thus, all CIPO included in this study were idiopathic in origin; patients with CIPO secondary to known genetic abnormalities were excluded. Anorexia nervosa was specifically excluded in all patients with malnutrition by a psychiatric examination. The clinical diagnosis of idiopathic CIPO was established on the basis of a chronic (>3 months), severe symptom complex mimicking mechanical small bowel obstruction, and (at least on one occasion) radiological evidence of air-fluid levels or dilated small bowel loops. All the experimental procedures were approved by the Ethics Committees of the Vall d'Hebron Hospital and St. Orsola-Malpighi Hospital for handling and analysis of tissue samples from patients with severe gut dysmotility (EM/146/2014/O). Tissue specimens from each patient were divided in 2 portions: one was immediately fixed in cold neutral 4% formaldehyde, and the other snap frozen in liquid nitrogen and stored –80°C.

2.2 Clinical features of patients with CIPO

Prior to laparoscopic surgery for tissue collection, patients completed a clinical questionnaire reporting the following data, symptoms and signs: age, sex, BMI, symptoms onset, number of sub-occlusive episodes that occurred prior to the surgery, abdominal distension, abdominal pain, nausea, vomiting, fullness, early satiety, constipation, diarrhea, esophageal involvement (i.e. motor abnormalities assessed by standard esophageal manometry), gastroparesis (established by scintigraphic gastric emptying), small intestine bacterial overgrowth (SIBO) (determined by glucose/lactulose breath test), urinary symptoms and small bowel dilation (detectable at abdominal CT-scan or MRI). Medications used by each subject were recorded.

2.3 Samples preparation and immunohistochemistry (IHC)

Specimens were fixed in 4% paraformaldehyde (Merck KGaA, Darmstadt, Germany), paraffin-embedded, cut into 5-μm-thick sections and mounted serially on poly-L-lysine-coated slides (Thermo Fisher Scientific, Rockford, USA). Before use, slides were deparaffinized in xylene, dehydrated through graded ethanol (both from Merck KGaA, Darmstadt, Germany), and washed thoroughly in phosphate buffer saline (137mM NaCl, 0.27×10^{-3} % 2mM KH_2PO_4; 10mM Na_2HPO_4; pH 7.4, all salts purchased from Merck KGaA, Darmstadt, Germany). To provide an adequate assessment of the neuromuscular component, sections were processed for histochemical and immunohistochemical analysis as established by guidelines from an International working team[9, 26] and applied in a recently published paper[27]. Antisera were used to identify different components of the gut tissue with HRP/DAB standard method using the immunoperoxidase secondary detection system IHC Select HRP/DAB (Merck KGaA, Darmstadt, Germany). Antibodies were diluted as follow: rabbit polyclonal anti-neuron-specific enolase (NSE; PA5–12374 Thermo Fisher Scientific, Rockford, USA) 1:1 and rabbit polyclonal anti-synaptophysin (A0010)* 1:100, both paneuronal markers; rabbit polyclonal anti-S100β (Z0311)* 1:400, to detect glial cells. C-Kit rabbit polyclonal C-Kit / CD117 (A4502)* 1:400 for ICC immunolabeling. Mouse polyclonal antibodies to α-smooth muscle actin (α-SMA; M0851)*; 1:400, and mouse anti-BCL-2 oncoprotein clone 124 (BCL-2; M0887)* 1:100 were used for smooth muscle cell immunostaining and as a marker of neuronal survival, respectively. Mouse anti- CD45R0 clone OPD4 (M0834)* 1:50, and mouse anti-CD8 clone C8/144B (M 7103)* 1:25 were used

to identify leukocytes, T-helper and -suppressor lymphocytes, respectively. Finally, a mouse anti-mast cell tryptase clone AA1 (M7052)* 1:800 was used to detect mast cells. Each antibody specificity was proved by secondary antibody omission and immunoblocking experiments. *These antibodies were purchased from Dako, Glostrup, Denmark.

2.4 Mast cell count

Two sections for each patient were stained using mast cells tryptase antibody (1:800). Random fields (n= 8 each) for mucosa, sub-mucosa, and neuromuscular layer have been captured with a Nikon Dxm 1200 camera connected to an Olympus AX 70 microscope, 400X final magnification. (Olympus, Melville, NY, USA). The specific area of tissue has been calculated using imageJ 1.48v free software that is an open source program from the National Institute of Health, Bethesda, MD, USA., discarding empty spaces. Mast cells were expressed as total number / mm^2 of each layer.

2.5 Patient sub-group classification

Within the n= 22 enrolled CIPO patients we recognized three histopathological patterns according to the London classification[6] and already described by our group;[27] briefly:

I. Apparently normal (AN) (n=5; age range: 29–61; 3 females), i.e. patients with no detectable changes of cellular components or inflammation in the neuromuscular layer. The other 17 patients showed ganglionic and/or muscular abnormalities with or without an inflammatory infiltrate (mainly mast cells) throughout the neuromuscular layer. Specifically:

II. Inflammatory neuro-myopathy (INF) (n=8; age range: 16–77; 5 females) characterized by an inflammatory infiltrate in the neuromuscular layer (lymphocytes, eosinophils and mast cells in 2 male patients and a predominant mast cell infiltrate in the remaining 6 patients). Specifically, mast cell count/mm^2 of INF was 117.3±90.8, whereas it was undetectable in controls and the other two subsets (S1 Fig 1.).

III. Degenerative neuro-myopathy (DEG) (n=9; age range: 32–75; 4 females) showed major neuronal and/or muscular structural/molecular changes identifiable at or routine histopathology or immunohistochemistry.

2.6 Protein expression

Total proteins were extracted from 0.5 g of each jejunal sample using TPER tissue protein extraction reagent in the presence of protease inhibitor cocktail (Thermo Fisher Scientific, Rockford, USA). Total protein fractions were quantified using a NanoDrop 2000 spectrophotometer (Thermo Fisher Scientific, Rockford, USA) and were stored at –80°C.

All proteins investigated in this study were separated using SDS-PAGE technique under reducing condition. Total protein content and the concentration of acrylamide used for each investigated protein are indicated in Table 1 Samples were diluted (v/v) in home-made Laemmli sample buffer pH 6.8 (4% SDS; 20% Glycerol; 120 mM Tris-Cl; bromophenol blue 0.02% all purchased from Merck KGaA, Darmstadt, Germany) and boiled 10 min before loading onto gel. To detect OCLN/CLDNs oligomeric assembly, total protein extract

of each sample was separated also under non-reducing conditions as previously described.[12] Proteins were separated in a precast gel 4–20%. This technique allows the identification of oligomeric OCLN/CLDNs complex (>150 KDa), and dimeric (OCLN$_D$ ~110–120 KDa), or monomeric (OCLN$_M$ 53–65 KDa) or low molecular weight (OCLN$_{LMW}$ 37–25 KDa) OCLN forms. Proteins were transferred onto nitrocellulose membrane (Thermo Fisher Scientific, Rockford, USA) overnight at 12 mV. Membranes were blocked with a buffer containing 5% fat-free milk (Merck KGaA, Darmstadt, Germany) and then incubated overnight at 4 °C respectively with the specific antibody. Membranes were washed three times in phosphate Tris buffer saline (100mM Tris HCl, 1.5M NaCl, 0.5% Tween-20, pH 8.3 all purchased from Merck KGaA, Darmstadt, Germany) and incubated with the specific HRP-conjugated secondary antibody (HRP conjugated secondary antibody: anti-mouse and anti-rabbit were from Sigma, Darmstadt, Germany, anti-goat was from Bethyl Laboratories, Montgomery, TX, USA) 2 hours at room temperature. Immunoreactive bands were visualized by ECL Western Blotting Substrate (Thermo Fisher Scientific, Rockford, USA) on a C-DiGit Blot Scanner system and quantified by the dedicated software Image Studio Software version 3.1.4 (LI-COR, Bad Homburg, Germany). Band intensities were expressed relative to the intensity of reference protein (GAPDH or Vinculin) detected on the same membrane following stripping with Restore Plus Western Blot Stripping Buffer (Thermo Fisher Scientific, Rockford, USA). OCLN/CLDNs complexes were only qualitatively considered (i.e., as 'absent' or 'present') and not quantified because of the low signal associated to OCLN/CLDNs complexes (bands >150 KDa) and the inter-patient variability of the specific band pattern. Each sample was run in duplicate in the same membrane and each assay was conducted in duplicate on separate membranes.

Rabbit polyclonal anti occludin (711500) and mouse monoclonal anti-claudin-4 (329400) were purchased from Thermo Fisher Scientific, Rockford, USA. Rabbit polyclonal anti-ZO-1 antibody (GTX108613) and rabbit polyclonal anti-vinculin antibody (GTX113294) were purchased from GeneTex, Inc. San Antonio, Texas, USA. Rabbit polyclonal anti-VIP (H-95) (sc-20727) was obtained from La Santa Cruz Biotechnology, Inc. Heidelberg Germany. Rabbit polyclonal anti-GFAP (Z0334) were obtained from Dako, Glostrup, Denmark Mouse anti-GAPDH clone 6C5 (ab8245) was purchased from Abcam, Cambridge, UK.

2.7 Statistical analysis

Differences in protein expression and mast cell abundance among groups were evaluated using Student's t test. The presence/absence of OCLN/CLDNs oligomers have been tested using Fisher test. The Spearman correlation test has been used to assess the possible correlation between biochemical parameters or with patients' symptoms and signs.

3. RESULTS

3.1 Evaluation of symptoms and signs

Symptoms, signs as well as main presenting clinical findings of CIPO patients are reported in Table 2 The three patient subsets, i.e. those with AN, INF and DEG histopathological patterns did not show significant differences in terms of clinical features.

3.2 OCLN expression and assembly with CLDNs

$OCLN_{TOT}$ expression changes are reported in Fig 1A-C. A significant decrease (about 37%) of $OCLN_{TOT}$ was detected in CIPO compared to controls (98.8±39.2 *vs.* 159.6±56.7 A.U. ±SD; P=0.0035) (Fig 1A). Specifically, compared to controls $OCLN_{TOT}$ decrease was identified in AN (80.1±35.6 *vs.* 159.6±56.7 A.U.±SD; P=0.0349) and INF (85.2±42.5 *vs.* 159.6±56.7 A.U.±SD; P=0.0124), but not in DEG (116.3±35.3 *vs.* 159.6±56.7 A.U.±SD; P=ns) (Fig 1B, C).

OCLN/CLDN oligomerization, characterized by the evidence of high molecular weight bands (>150 KDa), was detected in all controls, whereas it was undetectable in 73% of CIPO (P=0.0005) (Fig 1D, E). Compared to controls, the loss of the oligomeric assembly was equally reduced in the AN, INF, and DEG subgroups (P=0.0008; P=0.0256 and P=0.009, respectively). Since not directly related to TJ pore structure, the data about the other forms of occludin detectable in non-reducing conditions (e.g., $OCLN_D$, $OCLN_M$ and $OCLN_{LMW}$) were not further detailed in this study. However, $OCLN_D$ and $OCLN_{LMW}$ did not change in CIPO and histopathologically related subgroups *vs.* controls, whereas $OCLN_M$ decreased only in AN (P= 0.0105) and INF (P= 0.0184) *vs.* controls (data not shown), reflecting $OCLN_{TOT}$ expression in these two subsets.

3.3 CLN4 expression

CLN4 protein expression (Fig 2A-C) showed a 2-fold increase in CIPO compared to controls (51.7±31.6 *vs.* 24.2±9.1 A.U±SD; P=0.0480). Compared to controls, CLN4 expression increased 2.2 and 2.5 folds in INF (53.0±26.2 *vs.* 24.2±9.1 A.U±SD; P=0.0250) and DEG (60.9±40.4 *vs.* 24.2±9.1 A.U±SD; P=0.0500), respectively, whereas did not differ significantly in AN despite an increasing trend (32.9±12.4 *vs.* 24.2±9.1 A.U±SD; P=ns).

3.4 ZO-1 expression

ZO-1 protein expression (Fig 3A-C) was not altered in CIPO overall (21.4±21.0 *vs.* 23.4±14.2 A.U.±SD; P=ns) either in the AN (43.9±24.3 *vs.* 23.4±14.2 A.U.±SD; P=ns) or INF (22.8±14.4 *vs.* 23.4±14.2 A.U.±SD; P=ns) subgroups compared to controls. However, there was a 2.8-fold decrease of ZO-1 protein content in DEG *vs.* controls (7.7±11.0 *vs.* 23.4±14.2 A.U.±SD; P=0.0260).

3.5 VIP expression

Similarly to ZO-1 results, VIP content (Fig 3D-F) did not change in CIPO overall (18.9±12.9 *vs.* 26.8±10.1 A.U±SD; P=ns) as well as in AN (16.5±17.1 *vs.* 26.8±10.1 A.U. ±SD; P=ns) and INF (23.4±13.5 *vs.* 26.8±10.1 A.U±SD; P=ns) subgroups compared to controls. By contrast, a 1.7-fold decrease of VIP protein content was detected in DEG *vs.* controls (15.8±9.8 *vs.* 26.8±10.1 A.U.±SD; P=0.0458).

3.6 GFAP expression

A 31-fold increase of GFAP expression (Fig 4A-C) was observed in CIPO *vs.* controls (547.5±674.4 *vs* 17.6±24.1A.U.±SD; P =0.0499). All subgroups exhibited a very strong glial activation resulting in an increased GFAP expression. Compared to controls, GFAP is

overexpressed 19, 15 and 52 folds in AN (344.2±318.1 *vs.* 17.6±24.1A.U.±SD; P=0.0201), INF (263.9±211.9 *vs.* 17.6±24.1A.U.±SD; P=0.0094) and DEG (912.6±920.9 *vs.* 17.6±24.1A.U.±SD; P=0.0231), respectively.

3.7 Mast cell count

The numbers of mast cells infiltrating the mucosa (Fig 5A-C) remained unaltered in CIPO (190.1±164.8) and in each subgroups (AN 79.8±59.7; INF 283.8±227.3; DEG 159.6±64.0) *vs* controls (99.3±64.5). Mast cells infiltrating the submucosa (Fig 5D-F) in CIPO displayed a 1.8-fold increase (91.2±57.6) *vs.* controls (49.6±37.2), although this change was not statistically significant. In the subgroup analysis, mast cells showed 2.7-fold increase in INF patients (134.7±50.9) *vs.* controls (P=0.0039). AN (30.1±36.2) and DEG (82.6±36.7) subgroups showed mast cell counts similar to controls.

3.8 Correlations

$OCLN_{TOT}$ expression positively correlated with OCLN/CLDN oligomeric assembly (R=0.50, *P*=0.0040). Tissue specimens displaying a higher content of tissue $OCLN_{TOT}$ had a lower CLDN4 expression (R=−0.4379, P=0.0198). There was a positive correlation between CLDN4 expression and GFAP expression (R=0.4109, P=0.0333). The increased expression of both CLDN4 and GFAP and the absence of oligomers correlated with an increased number of sub-occlusive episodes (R=0.4373, P=0.0255; R=0.7877, P>0.0001 and R=−0.4303, P=0.0223 respectively) and with abdominal distension (R= 0.5029, P=0.0088; R=0.7394, P>0.0001 and R=−0.5353, P=0.0033). Abdominal pain was associated with the loss of oligomeric assembly and with GFAP overexpression (R=−0.5119, P=0.0054 and R=0.6302; P=0.0004). The CIPO duration was associated to the loss of oligomeric assembly along with VIP downregulation and with GFAP overexpression (R=−0.4873, *P*=0.0099; R=−0.4354; P=0.0262; and R=0.6887; P=0.0001, respectively).

CVC infection occurrence correlated with the loss of oligomeric assembly and with VIP down regulation (R=−0.5667, P=0.0435 and R=−0.6411; P=0.0247). SIBO correlated with ZO-1 down regulation and with CLDN4 overexpression (R=−0.4261; P=0.0238 and 0.4689; P=0.0157).

In INF subgroup, the increased number of mast cell infiltrating the submucosa correlated with oligomer loss (R=−0.7452, P=0.0022). Furthermore, mast cell density in the submucosa and in the neuromuscular layer correlated with an increased expression of GFAP (R=0.7802, P=0.0353 and R=0.7800, P=0.0017), an increased number of sub-occlusive episodes (R=0.8021, P=0.0006 and R=0.8717, P<0.0001), increased abdominal distension (R=0.7619, P=0.0015 and R=0.8880, P<0.0001), abdominal pain (R=0.6841, P=0.0070 and R=0.8510, P=0.0001), as well as with the duration of CIPO (R=0.6391, P=0.0187 and R=0.7680, P=0.0022). In DEG, ZO-1 downregulation correlated with GFAP upregulation (R=−0.5460, P=0.0287).

4. DISCUSSION

Changes in IEVB structure have been documented in a variety of conditions ranging from inflammatory diseases, such as inflammatory bowel disease, celiac disease and enteric

infection, to functional bowel disorders, e.g. irritable bowel syndrome. Even extra-GI disorders, such as diabetes mellitus and autoimmune disorders, may also show abnormalities to IEVB structure and function.[24] Although neuro-ICC-muscular abnormalities represent a major factor in the pathogenesis of gut dysfunction and symptom generation in CIPO,[4, 7-9] the role of enteric luminal mechanisms, and in particular of IEVB, has never been explored in such patients. In this study we addressed whether changes of TJ components occur in CIPO, and the possible correlations of identified IEVB -related molecular changes to main clinical features and investigated the possible implication of mast cell infiltration, glial activation, VIP expression in IEVB integrity.

Using non-reducing conditions, which allow for the separation and maintenance of multimeric structure of proteins, and a gradient gel, we were able to detect the different OCLN/OCLN and OCLN/CLDNs assembly. With this method, we discovered that oligomers, a key feature of TJ assembly and IEVB integrity, are not detectable in 73% of CIPO patients, regardless of their histopathological phenotypes. OCLN assembles into homo- or hetero-dimers or higher order oligomers with CLDNs to form the selective TJ pore located in the apical side of enterocytes[13] or in the endothelium of blood vessels.[28] Thus, our data indicate that the first gates of paracellular permeability are altered in most CIPO patients, thereby allowing endoluminal *noxae* come across and interact with various cellular components, e.g. immunocytes, of deeper GI layers. A significant decrease in $OCLN_{TOT}$ content was observed in AN and INF CIPO subsets. In patients with DEG alterations, we observed a specific reduction of ZO-1 protein, which, conversely, remains unchanged in the other two subgroups. Since the pore stability is essential for TJ function and is influenced by all the intra- or extra-cellular components that form the TJ,[12, 29, 30] our data suggest that oligomers assembly was altered in most CIPO although arising from different pathways, i.e. OCLN or ZO-1 downregulation, depending on the histopathological features. Some differences did not reach statistical significance because of the small size of the different subgroups investigated in this study, which dealt with a very rare condition such as CIPO.

There is association between CIPO patients with INF feature and $OCLN_{TOT}$ loss, without alteration in ZO-1expression. This pattern is in line with previously published observations on a wide array of GI and extra-GI inflammatory conditions.[31-35] McDermott et al. demonstrated that the nematode *T. spiralis* infection in the mouse model increased jejunal paracellular permeability and decreased OCLN expression in TJs. Furthermore, they demonstrated that c-kit-positive mast cells in IL-9 transgenic mice were directly responsible for the increase in epithelial paracellular permeability, whereas mast cell-specific protease deficient mice failed to show an increased intestinal permeability.[33] These experimental data are in line with our findings in the subset of patients with INF features, showing the correlation between decreased $OCLN_{TOT}$ expression and increased submucosal mast cell number. Furthermore, when mast cells infiltrate the submucosa and neuromuscular layer in this subgroup, GFAP expression increased, which reflects glial cell activation. In another study, Kucharzik et al. performed an immunofluorescence analysis revealing an overall downregulation of OCLN (but not ZO-1, CLDN1 or cell adhesion proteins) in the mucosa of patients with ulcerative colitis, a finding detectable in areas with active inflammation as well as in the mucosa uninvolved by the inflammatory insult.[34] This latter feature is reminiscent

of our data showing $OCLN_{TOT}$ downregulation in the sub-group with AN features, which exhibits no alterations in the neuro-muscular layer integrity.

We observed a selective reduction of ZO-1 expression in patients with DEG alterations, without changes in OCLN protein expression, but involving VIP, a well-known neuromodulator / neurotransmitter in the ENS. A prior study by Neunlist et al. had shown in a human HT29-C1.16E and Caco-2 co-culture model that VIP released by submucosal neurons restored IEVB functional integrity by increasing ZO-1 mRNA expression and protein content.[8] In line with these data, we specifically observed in the DEG subgroup concomitant downregulation in ZO-1 and VIP suggesting that neuronal mechanisms may contribute to TJ assembly via regulation of ZO-1 expression. In parallel, these data may help to understand the significance of ZO-1 changes in pathological conditions, such as blood-brain-barrier dysfunction as observed in patients with neurological disorders including multiple sclerosis and Alzheimer's disease.[36]

All CIPO subgroups had in common a prominent increase of GFAP expression that was even more pronounced in the DEG subset, supporting the occurrence of marked glial cell activation. It has been demonstrated that GFAP-mediated glial hyper activation is associated with cytoskeletal disorganization,[37] and that this pathological mechanism occurs in degenerative diseases, i.e. Alzheimer's and frontotemporal dementia.[38] GFAP induced rearrangements/disintegration of the cytoskeleton, evoked astrocyte cell death and, as a result, a decreased blood-brain barrier function.[38] Savidge et al. demonstrated that glial cells can influence peri-junctional F-actin and its association with ZO-1, both mechanisms exerting a role in the maintenance of the enterocyte cytoskeleton and therefore IEVB stability.[39] Thus, an increased GFAP expression and the concomitant ZO-1 downregulation suggest the occurrence of a cytoskeletal disorganization, which contributes to IEVB abnormalities in patients with DEG changes. Furthermore, in subgroups with INF and DEG alterations, the GFAP increased expression is accompanied by CLDN4 upregulation. This finding is in line with previous observations by Horng et al. who showed that experimental glial cell activation (i.e., astrogliosis) is accompanied by upregulation of CLDN4 protein. These authors hypothesized that this effect could be a "protective mechanism" to seal cells in the absence of a physiological barrier.[40] Since the tissue specific composition of jejunal CLDNs in TJs is still unknown, whether CLDN4 overexpression can determine a modification on CLDNs stoichiometry at the TJ pore in CIPO patients remains to be proved. Our data indicated that a possible glial activation, as inferable by GFAP upregulation, along with CLDN4 overexpression and the loss of oligomers suggest more severe CIPO forms characterized by recurrent intestinal sub-occlusive episodes and marked abdominal distension. Further study will be needed to establish whether these protein expression abnormalities uncovered by our study are clinically relevant, for instance in predicting the severity of CIPO patients and their long term progression Another potentially important yield of the present study is the putative relationship between clinical manifestations (symptoms / signs) in patients with CIPO and the expression of proteins that regulate paracellular permeability.

The relevance of our study is underscored by the novel description of IEVB abnormalities in CIPO and represents the first step to clarify the biochemical mechanisms of a leaky gut in a

severe form of gut dysmotility such as CIPO. Considered in their entirety, our results point towards two different pathogenetic mechanisms that may alter the IEVB structure in CIPO. Some elements such as GFAP related glial cell activation, CLDN4 upregulation, and loss of oligomeric assembly, appear to be common to each of the investigated CIPO patient subgroups regardless of the underlying neuro-muscular abnormalities. Other mechanisms such as mast cells infiltrate, particularly throughout the submucosa, and the associated reduced OCLN expression may operate in the INF subgroup leading to TJ-related IEVB abnormalities. In the DEG subgroup VIP downregulation may primarily affect ZO-1 expression, thereby enterocyte cytoskeleton, which is a crucial factor for TJ core stability and IEVB integrity.[40] In the AN subgroup, OCLN decrease may occur as a primary step rather than as a consequence of inflammatory activity (mast cells) or other insults which have been identified to occur in IEVB changes detected in the other two subsets of CIPO patients. In conclusion this study demonstrated that the IEVB is impaired in idiopathic CIPO of either inflammatory or degenerative origin. The common feature is that TJ proteins lose their ability to form oligomers. However, the mechanisms by which oligomerization is impaired seem to be different among the various CIPO subgroups. Whereas in INF CIPO, mast cells and OCLN content appear to be key players in barrier structural alterations, in DEG forms the effects are due to cytoskeleton changes induced by GFAP overexpression and the simultaneous VIP-associated ZO-1 downregulation. The relative contribution of the several molecular and cellular factors identified in this study on CIPO patients and related subsets remains to be established. Further studies will be necessary to clarify the pathogenetic role of IEVB alterations in the development of various intestinal dysfunctions associated with CIPO. Nonetheless, this study provides a framework for a better pathophysiological understanding of severe changes in digestive motility and may contribute to the development of new therapies targeting changes of IEVB.

Supplementary Material

Refer to Web version on PubMed Central for supplementary material.

Acknowledgments

REFERENCES

1. Cogliandro RF, Antonucci A, De Giorgio R, et al. Patient-reported outcomes and gut dysmotility in functional gastrointestinal disorders. Neurogastroenterol Motil 2011;23:1084–91. [PubMed: 21917083]

2. Lindberg G, Tornblom H, Iwarzon M, et al. Full-thickness biopsy findings in chronic intestinal pseudo-obstruction and enteric dysmotility. Gut 2009;58:1084–90. [PubMed: 19136514]

3. De Giorgio R, Sarnelli G, Corinaldesi R, et al. Advances in our understanding of the pathology of chronic intestinal pseudo-obstruction. Gut 2004;53:1549–52. [PubMed: 15479666]

4. De Giorgio R, Cogliandro RF, Barbara G, et al. Chronic intestinal pseudo-obstruction: clinical features, diagnosis, and therapy. Gastroenterol Clin North Am 2011;40:787–807. [PubMed: 22100118]

5. Tornblom H, Lang B, Clover L, et al. Autoantibodies in patients with gut motility disorders and enteric neuropathy. Scand J Gastroenterol 2007;42:1289–93. [PubMed: 17918010]

6. Knowles CH, De Giorgio R, Kapur RP, et al. The London Classification of gastrointestinal neuromuscular pathology: report on behalf of the Gastro 2009 International Working Group. Gut 2010;59:882–7. [PubMed: 20581236]

7. Knowles CH, Lindberg G, Panza E, et al. New perspectives in the diagnosis and management of enteric neuropathies. Nat Rev Gastroenterol Hepatol 2013;10:206–18. [PubMed: 23399525]

8. Neunlist M, Toumi F, Oreschkova T, et al. Human ENS regulates the intestinal epithelial barrier permeability and a tight junction-associated protein ZO-1 via VIPergic pathways. Am J Physiol Gastrointest Liver Physiol 2003;285:G1028–36. [PubMed: 12881224]

9. Keller J, Bassotti G, Clarke J, et al. Expert consensus document: Advances in the diagnosis and classification of gastric and intestinal motility disorders. Nat Rev Gastroenterol Hepatol 2018;15:291–308. [PubMed: 29622808]

10. Spadoni I, Zagato E, Bertocchi A, et al. A gut-vascular barrier controls the systemic dissemination of bacteria. Science 2015;350:830–4. [PubMed: 26564856]

11. Chiba H, Osanai M, Murata M, et al. Transmembrane proteins of tight junctions. Biochim Biophys Acta 2008;1778:588–600. [PubMed: 17916321]

12. McCaffrey G, Willis CL, Staatz WD, et al. Occludin oligomeric assemblies at tight junctions of the blood-brain barrier are altered by hypoxia and reoxygenation stress. J Neurochem 2009;110:58–71. [PubMed: 19457074]

13. McCaffrey G, Seelbach MJ, Staatz WD, et al. Occludin oligomeric assembly at tight junctions of the blood-brain barrier is disrupted by peripheral inflammatory hyperalgesia. J Neurochem 2008;106:2395–409. [PubMed: 18647175]

14. Turksen K, Troy TC. Barriers built on claudins. J Cell Sci 2004;117:2435–47. [PubMed: 15159449]

15. Van Itallie CM, Fanning AS, Anderson JM. Reversal of charge selectivity in cation or anion-selective epithelial lines by expression of different claudins. Am J Physiol Renal Physiol 2003;285:F1078–84. [PubMed: 13129853]

16. Barmeyer C, Schulzke JD, Fromm M. Claudin-related intestinal diseases. Semin Cell Dev Biol 2015;42:30–8. [PubMed: 25999319]

17. Van Itallie CM, Fanning AS, Bridges A, et al. ZO-1 stabilizes the tight junction solute barrier through coupling to the perijunctional cytoskeleton. Mol Biol Cell 2009;20:3930–40. [PubMed: 19605556]

18. Zlokovic BV. The blood-brain barrier in health and chronic neurodegenerative disorders. Neuron 2008;57:178–201. [PubMed: 18215617]

19. Shen L Tight junctions on the move: molecular mechanisms for epithelial barrier regulation. Ann N Y Acad Sci 2012;1258:9–18. [PubMed: 22731710]

20. Turner JR. Intestinal mucosal barrier function in health and disease. Nat Rev Immunol 2009;9:799–809. [PubMed: 19855405]

21. Krause G, Winkler L, Mueller SL, et al. Structure and function of claudins. Biochim Biophys Acta 2008;1778:631–45. [PubMed: 18036336]

22. Lelievre V, Favrais G, Abad C, et al. Gastrointestinal dysfunction in mice with a targeted mutation in the gene encoding vasoactive intestinal polypeptide: a model for the study of intestinal ileus and Hirschsprung's disease. Peptides 2007;28:1688–99. [PubMed: 17606312]

23. Conlin VS, Wu X, Nguyen C, et al. Vasoactive intestinal peptide ameliorates intestinal barrier disruption associated with Citrobacter rodentium-induced colitis. Am J Physiol Gastrointest Liver Physiol 2009;297:G735–50. [PubMed: 19661153]

24. Savidge TC, Sofroniew MV, Neunlist M. Starring roles for astroglia in barrier pathologies of gut and brain. Lab Invest 2007;87:731–6. [PubMed: 17607301]

25. Pekny M, Nilsson M. Astrocyte activation and reactive gliosis. Glia 2005;50:427–34. [PubMed: 15846805]

26. Knowles CH, De Giorgio R, Kapur RP, et al. Gastrointestinal neuromuscular pathology: guidelines for histological techniques and reporting on behalf of the Gastro 2009 International Working Group. Acta Neuropathol 2009;118:271–301. [PubMed: 19360428]

27. Malagelada C, Karunaratne TB, Accarino A, et al. Comparison between small bowel manometric patterns and full-thickness biopsy histopathology in severe intestinal dysmotility. Neurogastroenterol Motil 2018;30.

28. Spadoni I, Pietrelli A, Pesole G, et al. Gene expression profile of endothelial cells during perturbation of the gut vascular barrier. Gut Microbes 2016;7:540–548. [PubMed: 27723418]

29. McCaffrey G, Staatz WD, Quigley CA, et al. Tight junctions contain oligomeric protein assembly critical for maintaining blood-brain barrier integrity in vivo. J Neurochem 2007;103:2540–55. [PubMed: 17931362]

30. McCarthy KM, Skare IB, Stankewich MC, et al. Occludin is a functional component of the tight junction. J Cell Sci 1996;109 (Pt 9):2287–98. [PubMed: 8886979]

31. Antonetti DA, Barber AJ, Khin S, et al. Vascular permeability in experimental diabetes is associated with reduced endothelial occludin content: vascular endothelial growth factor decreases occludin in retinal endothelial cells. Penn State Retina Research Group. Diabetes 1998;47:1953–9. [PubMed: 9836530]

32. Yoshida Y, Morita K, Mizoguchi A, et al. Altered expression of occludin and tight junction formation in psoriasis. Arch Dermatol Res 2001;293:239–44. [PubMed: 11409568]

33. McDermott JR, Bartram RE, Knight PA, et al. Mast cells disrupt epithelial barrier function during enteric nematode infection. Proc Natl Acad Sci U S A 2003;100:7761–6. [PubMed: 12796512]

34. Kucharzik T, Walsh SV, Chen J, et al. Neutrophil transmigration in inflammatory bowel disease is associated with differential expression of epithelial intercellular junction proteins. Am J Pathol 2001;159:2001–9. [PubMed: 11733350]

35. Fries W, Mazzon E, Squarzoni S, et al. Experimental colitis increases small intestine permeability in the rat. Lab Invest 1999;79:49–57. [PubMed: 9952110]

36. Reinhold AK, Rittner HL. Barrier function in the peripheral and central nervous system-a review. Pflugers Arch 2017;469:123–134. [PubMed: 27957611]

37. Chen MH, Hagemann TL, Quinlan RA, et al. Caspase cleavage of GFAP produces an assembly-compromised proteolytic fragment that promotes filament aggregation. ASN Neuro 2013;5:e00125.

38. Mouser PE, Head E, Ha KH, et al. Caspase-mediated cleavage of glial fibrillary acidic protein within degenerating astrocytes of the Alzheimer's disease brain. Am J Pathol 2006;168:936–46. [PubMed: 16507909]

39. Savidge TC, Newman P, Pothoulakis C, et al. Enteric glia regulate intestinal barrier function and inflammation via release of S-nitrosoglutathione. Gastroenterology 2007;132:1344–58. [PubMed: 17408650]

40. Horng S, Therattil A, Moyon S, et al. Astrocytic tight junctions control inflammatory CNS lesion pathogenesis. J Clin Invest 2017;127:3136–3151. [PubMed: 28737509]

KEY POINTS

- Chronic intestinal pseudo-obstruction (CIPO) is a rare form of severe impairment of gut motility mainly due to neuro-interstitial cells of Cajal (ICC)-muscular abnormalities. Intestinal epithelial and vascular barrier (IEVB) changes, leading to a 'leaky gut', are known to contribute to a variety of pathological conditions, such as inflammatory and functional bowel disorders. However, whether IEVB changes occur in CIPO, thereby contributing to pathophysiology and clinical features, remain unclear.

- The abnormalities to protein expression and aggregation of major tight junction (TJ) components in the jejunum of CIPO patients suggest that IEVB integrity is compromised in CIPO.

- We propose that IEVB changes may contribute to neuro-ICC-muscular abnormalities in symptoms / manifestations detectable in CIPO patients. The identified molecular targets can be possibly exploitable to design treatment options for patients with severe gut dysmotility.
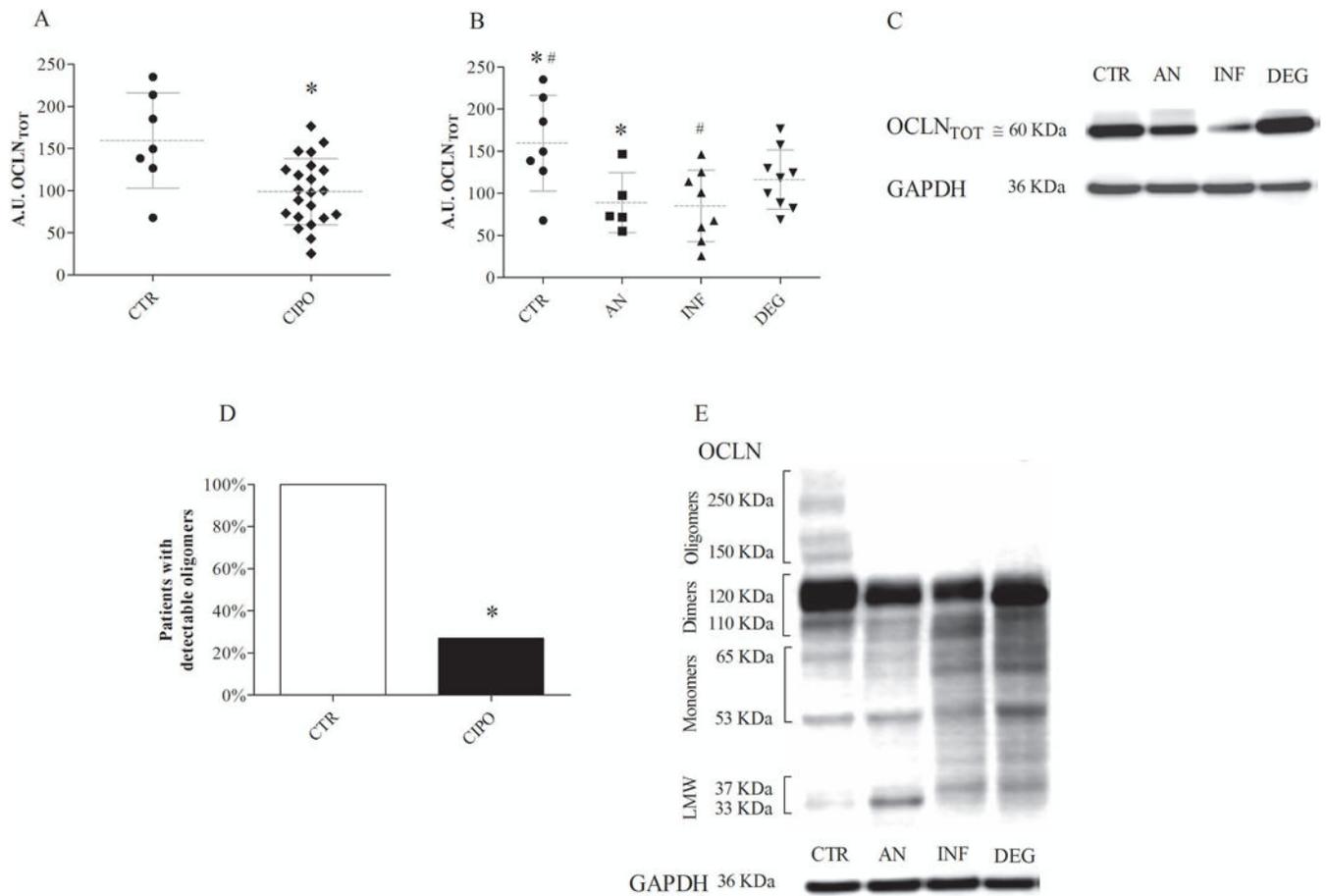
Fig 1. OCLN expression and OCLN/CLDN oligomeric assembly. OCLN$_{TOT}$ expression
A) in CIPO *P=0.0035; and **B)** in immunohistochemically defined subgroups *P=0.0349;
$^{\#}$P=0.0124. The same symbol superscript in the column indicates the pair with a statistically
significant difference. **C)** Example of WB separation and detection of OCLN$_{TOT}$
densitometry and reference protein GAPDH. **D)**. Representation of the percentage of
patients with oligomeric assembly detectable using WB (densitometric bands > 220 KDa)
*P=0.0005. **E)** Example of WB separation under non-reducing condition using a
polyacrylamide gradient gel 4–20% and reference protein GAPDH.
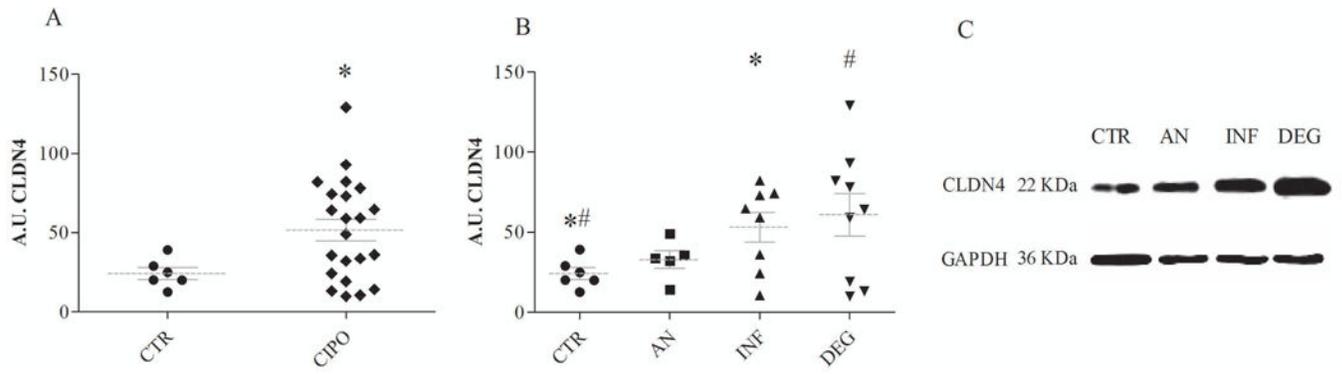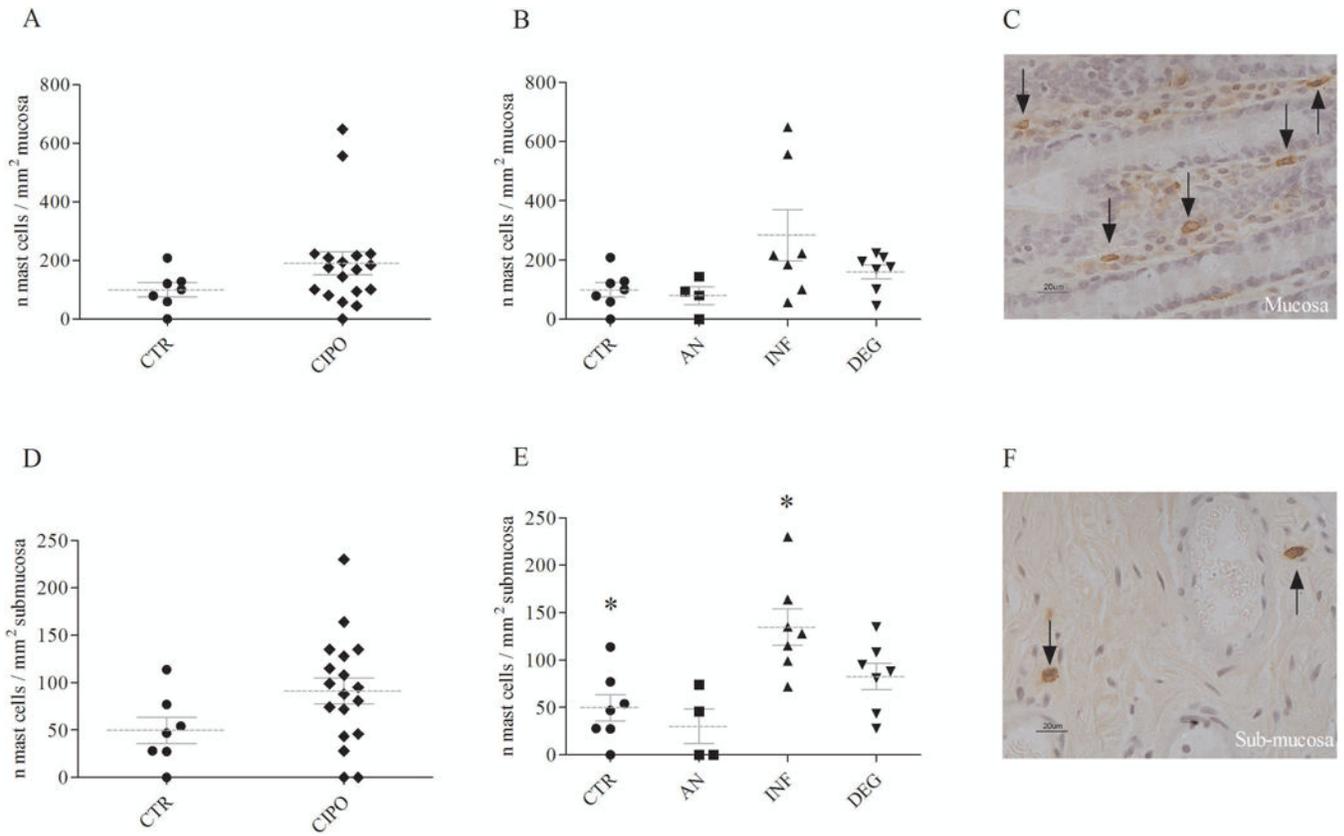
Fig 2. CLDN4 expression.
CLDN4 expression: **A)** in CIPO *P=0.0480; and **B)** in IHC subgroups *P=0.0250;
#P=0.0500. The same symbol superscript in the column indicates the pair with a statistically significant difference. **C)** Example of WB separation and detection of CLDN4 densitometry and reference protein GAPDH.
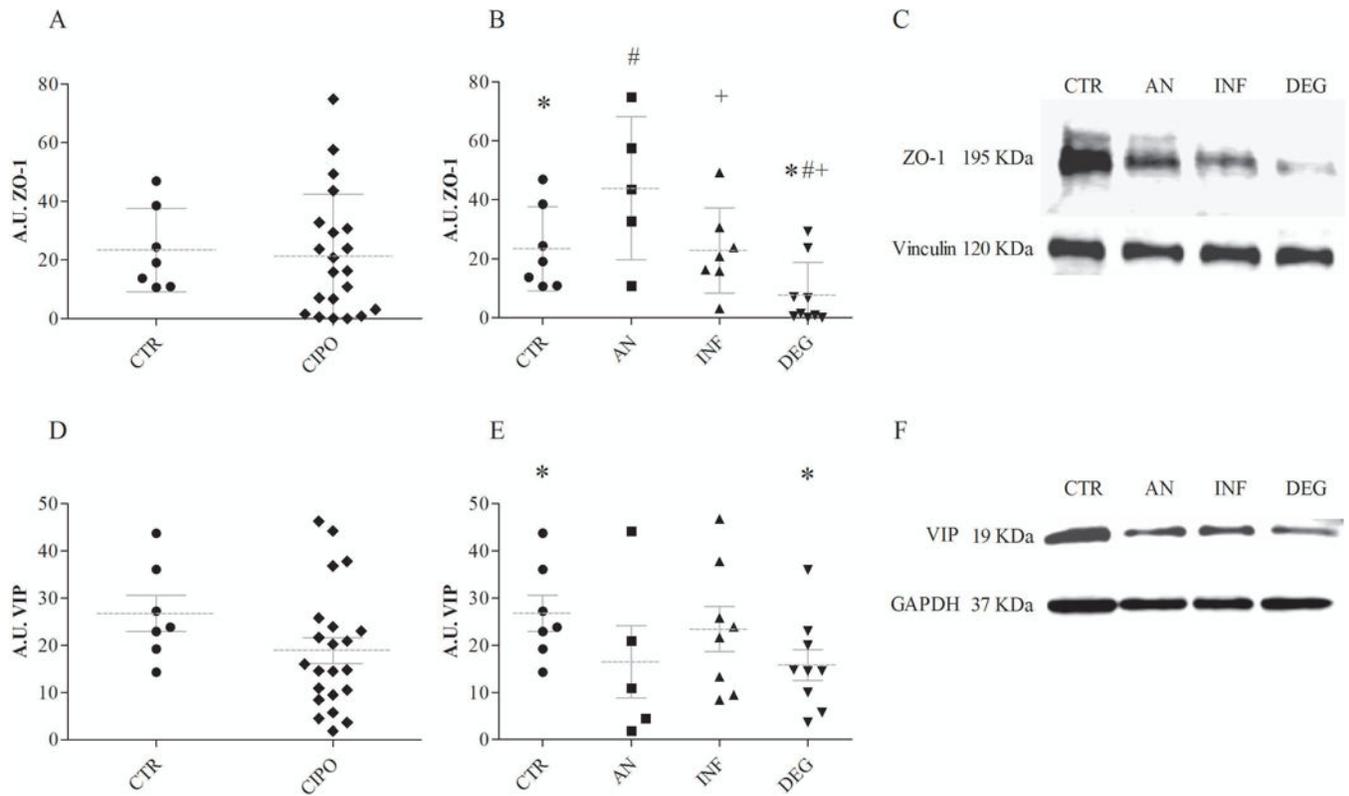
Fig 3. ZO-1 and VIP protein expression and correlation.
ZO-1 protein expression **A)** in CIPO; and **B)** in immunohistochemically defined subgroups
*P=0.0260; #P=0.0022 +P=0.0324; the same symbol superscript in the column indicates the
pair with a statistically significant difference. **C)** Example of WB separation and detection of
ZO-1 densitometry *vs.* vinculin reference protein signal. VIP protein expression **D)** in CIPO;
and **E)** in immunohistochemically defined subgroups *P=0.0305; the same symbol
superscript in the column indicates the pair with a statistically significant difference. **E)**
Example of WB separation and detection of VIP densitometry *vs.* GAPDH reference protein
signal.

Fig 4. GFAP protein expression.
GFAP expression **A)** in CIPO *P=0.0499; and **B)** in immunohistochemically defined subgroups *P=0.0201; #P=0.0094; +P=0.0231; the same symbol superscript in the column indicates the pair with a statistically significant difference. **C)** Example of WB separation and detection of GFAP densitometry *vs.* the specific reference protein GAPDH.

Fig 5. Mast cells quantitative analysis.
Mast cells counted per mm^2 of mucosa have been quantified **A)** in CIPO; and **B)** in IHC subgroups; **C)** Example of tryptase positive cells infiltrating the mucosa. Mast cells counts are expressed per mm^2 of sub-mucosa **D)** in CIPO; and **E)** in IHC subgroups ***P=0.0039**; the same symbol superscript in the column indicates the pair with a statistically significant difference. **F)** Example of tryptase positive cells infiltrating the sub-mucosa.

Table 1.

Tecnical information regarding the specific protein detection via WB tecnique.

Protein		MW (KDa)	Total protein amount (µg)	Acrylamide concentration	Antibody concentration	Reference protein
OCLN		60	20	12%		
OCLN assembly	Oligomers	>150	40	4 – 20%	2 µg/ml	GAPDH
	Dimers	110–120				
	Monomers	53–65				
	LMW	37–35				
CLDN4		22	100	15%	2 µg/ml	GAPDH
ZO-1		195	20	5%	1:500	Vinculin
VIP		19	100	15%	1:200	GAPDH
GFAP		50	100	15%	1:3000	GAPDH
GAPDH		36	20; 40; 100	12; 15; 4–20%	1:1000	-
Vinculin		129	20	5%	1:1000	-

Table 2.

Clinical manifestations of CIPO patients.

Symptoms and signs	Affected patients (%)
Abdominal distension	95 %
Abdominal pain	85 %
Constipation	60 %
Fullness	42 %
Early satiety	55 %
SIBO	45 %
Nausea	35 %
Delayed gastric emptying	35 %
Vomiting	25 %
Diarrhea	35 %
CVC infections	14 %
Small bowel dilatation	26 %
Esophageal involvement	20 %
Urinary symptoms	10 %
≥2 sub-occlusive episodes	80 %
Single sub-occlusive episode	20 %